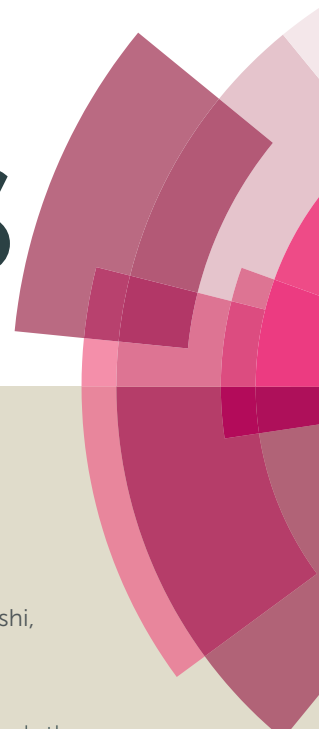


RSC Advances



This article can be cited before page numbers have been issued, to do this please use: S. L. Jain, C. Joshi, P. Kumar, B. behera, A. Barras, S. Szunerits and R. Boukherroub, *RSC Adv.*, 2015, DOI: 10.1039/C5RA19466K.



This is an *Accepted Manuscript*, which has been through the Royal Society of Chemistry peer review process and has been accepted for publication.

Accepted Manuscripts are published online shortly after acceptance, before technical editing, formatting and proof reading. Using this free service, authors can make their results available to the community, in citable form, before we publish the edited article. This *Accepted Manuscript* will be replaced by the edited, formatted and paginated article as soon as this is available.

You can find more information about *Accepted Manuscripts* in the [Information for Authors](#).

Please note that technical editing may introduce minor changes to the text and/or graphics, which may alter content. The journal's standard [Terms & Conditions](#) and the [Ethical guidelines](#) still apply. In no event shall the Royal Society of Chemistry be held responsible for any errors or omissions in this *Accepted Manuscript* or any consequences arising from the use of any information it contains.

Cite this: DOI: 10.1039/c0xx00000x

www.rsc.org/xxxxxx

ARTICLE TYPE

Graphene/hemin hybrid material as efficient green catalyst for stereoselective olefination of aldehydes

Chetan Joshi,^a Pawan Kumar,^a Babita Behera,^b Alexandre Barras,^c Sabine Szunerits,^c Rabah Boukherroub^{c*} and Suman L. Jain^{a*}

Received (in XXX, XXX) Xth XXXXXXXXX 20XX, Accepted Xth XXXXXXXXX 20XX

DOI: 10.1039/b000000x

Hemin/graphene composite, prepared by mixing an aqueous solution of graphene oxide (GO) with hemin and sonicating the suspension for 5h at room temperature, was investigated for olefination of aldehydes using ethyl diazoacetate in the presence of triphenylphosphine. Efficient olefination of aromatic aldehydes with high (E)-selectivity was obtained, revealing that rGO/hemin is a promising heterogeneous catalyst for olefination reaction. The as-synthesized catalyst could easily be recovered from the reaction mixture and was subsequently used for several runs without any significantly loss in activity and selectivity.

Introduction

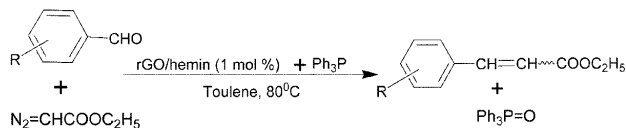
Olefination or construction of C=C double bonds is one of the most important transformations in synthetic organic chemistry. The Wittig reaction¹ is the most commonly and widely used approach for constructing carbon-carbon double bonds for a variety of applications. To avoid the basic conditions required for the generation of phosphorane precursors, an alternative methodology using easily accessible diazo compounds in the presence of metal complexes as catalysts has received considerable interest in recent decades.² Among the known metal complexes, iron macrocyclic complexes particularly iron porphyrins, phthalocyanines, and corroles displayed good catalytic activity for this olefination reaction.³ However, these catalysts suffer from the obvious drawbacks of the homogeneous catalysts such as difficult separation/recovery as well as non-recycling ability of the catalyst.

Hemin, a well-known porphyrinato iron complex, regarded as an active centre of various hem proteins such as hemoglobin, myoglobin etc,⁴ plays a vital key role in biochemical reactions and electron-transport chain. In addition, it has extensively been used as catalyst for various potential applications mainly related to environment and energy issues such as electrochemical reduction of nitrite,

nitric oxide, carbon dioxide, hydrogen peroxide and the oxidation of peroxyxynitrite.⁵ However, a serious drawback of hemin is its high instability due to oxidative degradation. It undergoes a self-oxidation into an inactive meso-hydroxyprophyrin form.⁶ Thus, a great number of efforts are being focused towards the structural modification of hemin in order to prevent its self-degradation.⁷ Although these modifications increase its activity and stability, they concurrently enhance synthetic difficulties and cost which make their utility limited for large scale applications. Alternatively, immobilization of hemin molecules to support materials constitutes a logical and promising approach to prevent their self-degradation. Furthermore, covalent or strong interaction of metalloporphyrin molecules to the support is advantageous as it prevents leaching and makes the catalyst more stable.

Graphene, a two dimensional single layered structure consisting of sp²-bonded carbon atoms has several distinctive properties such as extremely high electronic conductivity, superior mechanical strength, large surface area and highly conjugated structure.⁸ Owing to extraordinary physicochemical and structural properties, it has extensively been used as support for immobilizing organic and inorganic catalysts. The potential of graphene and reduced graphene oxide (rGO) to support organic molecules such as hemin and other porphyrin species through π - π stacking interactions has widely been investigated for electrocatalytic applications.⁹ However, their use as heterogeneous catalyst for organic transformations are rarely known.

In continuation of our on-going studies towards developing graphene-based hybrid catalysts for organic transformations, herein we report hemin functionalized reduced graphene oxide (rGO/hemin) hybrid material as an effective catalyst for olefination of aldehydes using ethyl diazoacetate (EDA) in presence of triphenylphosphine (TPP) as a reducing agent (Scheme 1). The developed heterogenized catalyst displayed comparable catalytic activity to the homogeneous iron porphyrin catalyst with the additional benefits of facile recovery and recycling (Table 1, entry 12).

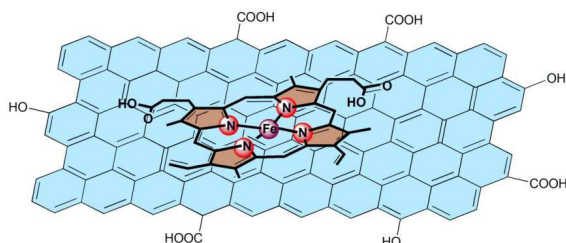


Scheme 1: Olefination of aldehydes

5 Results and discussion

Synthesis and characterization of the catalyst

Hemin (metalloporphyrin) being a flat molecule can readily be immobilized on the surface of rGO through π - π stacking and H-bonding interactions.¹⁰ The structure of rGO/hemin catalyst is illustrated in Scheme 2.



Scheme 2: Schematic illustration of rGO/hemin catalyst.

The detailed characterization of the synthesized material was reported in our previous report.¹¹ The incorporation of hemin onto rGO surface was confirmed by FTIR measurements (Fig. 1). The FTIR spectrum of hemin (Fig. 1a) showed characteristic absorption peaks at 1580–1600 cm^{-1} (benzenoid ring stretch) and 1100–1200 cm^{-1} (pyrrole vibration). The appearance of these characteristic bands in the FTIR spectrum of rGO/hemin clearly indicated that hemin molecules were successfully integrated to the rGO support.¹²

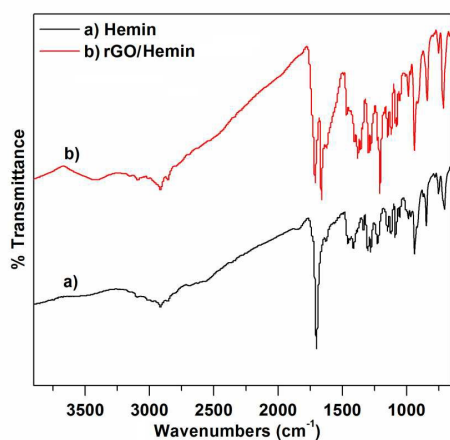


Fig. 1: FTIR spectra of a) hemin and b) rGO/hemin.

The morphology of the synthesized rGO/hemin catalyst was investigated using FE-SEM (Fig. 2). The appearance of

crumpled and erupted structure in the SEM image suggested the presence of reduced graphene oxide in rGO/hemin catalyst (Fig. 2a). EDX pattern of the synthesized composite confirmed the presence of iron (Fig. 2b). Further elemental mapping indicated the homogeneous distribution of iron throughout the catalyst (Fig. 2c, 2d).

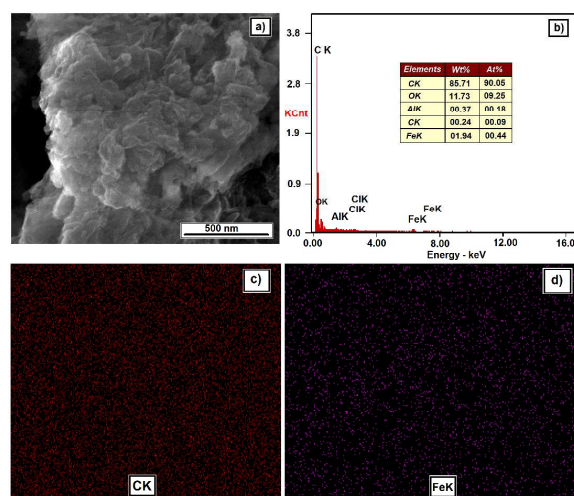


Fig. 2: rGO/hemin catalyst a) FE-SEM image, b) EDX pattern, and elemental mapping for (c) C, and d) Fe atoms.

The UV/Vis absorption spectra of hemin and rGO/hemin hybrid are displayed in Fig. 3. The spectrum of hemin in DMF shows characteristic absorption peaks i.e a strong absorption peak at 398 nm attributed to the Soret band and a broad hump between 450 and 650 nm corresponding to the Q-bands. The UV/Vis spectrum of rGO/hemin hybrid dispersed in DMF exhibits a broad absorption peak below and above 400 nm due to the ring π - π^* transitions of the Soret band of incorporated hemin. The changes observed in the Soret band in rGO/hemin hybrid confirmed the incorporation of hemin molecules within the rGO network.¹³

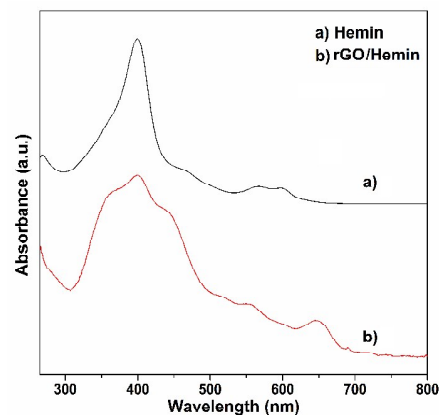


Fig. 3: UV-Vis spectra of a) hemin and b) rGO/hemin

Thermal stability of the synthesized materials was examined by thermogravimetric analysis (TGA) (Fig. 4). The TGA profile of rGO showed initial weight loss between 100–150 $^{\circ}\text{C}$ probably due to the evaporation of adsorbed water and solvent molecules. A very small weight loss between 400–600 $^{\circ}\text{C}$ was observed due to the loss of residual oxygen

carrying functionalities (Fig. 4a). In case of free hemin, a sharp weight loss occurred in the temperature range of 350–380 °C probably due to the degradation of the porphyrin ring structure (Fig. 4b). In contrast rGO/hemin hybrid exhibited two major weight losses; the first in the range of 100–150 °C due to adsorbed water molecules and another at 350 °C due to the degradation of the macrocyclic ring structure of the hemin (Fig. 4c).¹⁴

The iron content in the synthesized hybrid was found to be 6.8 wt % or 1.21 mmol/g cat as determined by ICP-AES analysis.

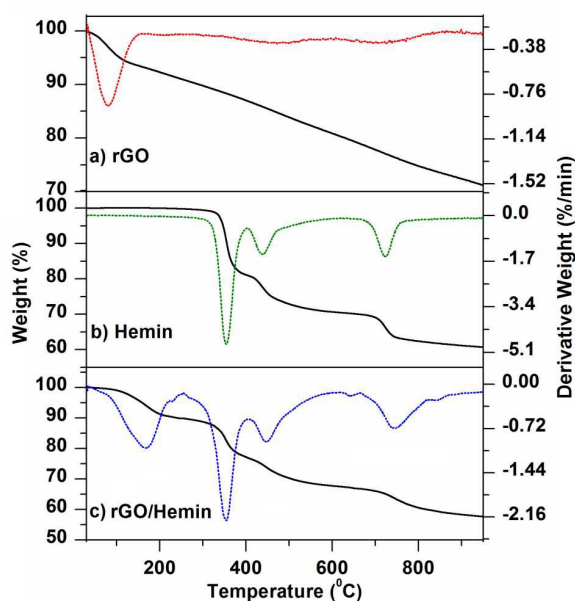


Fig. 4: DT-TGA thermograms of a) rGO, b) hemin and c) rGO/hemin

15 Catalytic activity

The catalytic activity of the rGO/hemin composite was investigated for the olefination of aldehydes using ethyl diazoacetate (EDA) in the presence of triphenylphosphine (PPh₃). At first the olefination of benzaldehyde (1 eq) with EDA (2 eq) in the presence of PPh₃ (1.1 eq) and rGO/hemin (1 mol %) was performed in toluene at 80 °C for 12 h. The reaction was found to occur efficiently and afforded olefination product in 92 % isolated yield with good *trans*-selectivity (Table 1, entry 4). In a control blank experiment, no olefination product was obtained in the absence of the catalyst (Table 1, entry 5). The presence of PPh₃ was found to be vital and in its absence conversion of benzaldehyde was not observed even after a prolonged reaction time (Table 1, entry 6). We also investigated the effect of various solvents such as toluene, dimethylformamide (DMF), dichloroethane (DCE) and THF on the reaction efficiency (Table 1, entries 1–4). Among all the solvents studied, toluene was found to be optimum for this chemical transformation. To establish the effect of catalyst amount on the product yield, we performed olefination of benzaldehyde under identical conditions by varying the catalyst amount from 1 to 5 mol % (Table 1, entries 4, 7–8). With increasing the amount of the catalyst, there was a slight increase in the

yield while the selectivity of the product remained unchanged. The reaction was found to be very slow at room temperature (Table 1, entry 9); the best results were obtained using toluene as solvent at 80 °C (entry 4). Further increase of the temperature to 100 °C did not show any significant enhancement in the conversion as well as selectivity (entry 10). Moreover, no reaction occurred when rGO was used as catalyst under described experimental conditions (Table 1, entry 11).

Table 1: Olefination of benzaldehyde under different reaction conditions^a.

Entry	Solvent	Catalyst amount (mol%)	Temperature (°C)	Yield (%) ^b	E/Z ratio ^c
1	THF	1	70	61	3:1
2	DMF	1	80	80	3:1
3	DCE	1	80	78	2.5:1
4	Toluene	1	80	92	4:1
5	Toluene	1	80	- ^d	-
6	Toluene	1	80	- ^e	-
7	Toluene	2	80	93	4:1
8	Toluene	5	80	93	4:1
9	Toluene	1	25	52	4:1
10	Toluene	1	100	94	4:1
11	Toluene	1	80	- ^f	-
12	Toluene	1	80	93 ^g	4:1

^aReaction condition: benzaldehyde (1 mmol), EDA (1.2 mmol); PPh₃ (1.1 mmol) under N₂ atmosphere; ^bIsolated yield; ^cdetermined by ¹H NMR; ^din the absence of catalyst; ^ein the absence of PPh₃; ^fusing rGO as catalyst; ^gusing homogeneous iron(II) porphyrin as catalyst.

To explore the scope of this reaction, a number of aldehydes were subjected to olefination under described reaction conditions (Table 2). As shown, all the substituted aldehydes reacted smoothly and gave the corresponding olefination products in moderate to high yields with high *trans*-selectivity. In general, among all the tested aryl aldehydes those containing electron-donating groups (Table 2, entries 2–5) were found to be comparatively more reactive and gave the desired olefin in high yields (85–94 %). Furthermore, the steric hindrance at ortho-position of aryl aldehydes (Table 2, entry 4) lowered the yield as well as *trans*-selectivity of the product. Interestingly, in case of benzaldehydes having electron withdrawing substituents the selectivity pattern of the product was found to be reversed and *cis*-olefins were formed predominantly (Table 2, entries 6–8). The exact reason for reversed regioselectivity in case of electron withdrawing substrates is not clear at this stage. A literature report by Shindo et al.¹⁵ suggested that the E/Z selectivity in the olefination reaction is strongly dependent on the electronic nature of the para-substituents. An increase of electron density on the phenyl substituents tends to increase the E-selectivity. However, the electron withdrawing substituents (particularly –NO₂ group) tend to give Z-olefins predominantly.

Highly hindered substrate like 2,4,6-trimethylbenzaldehyde did not give any product under the described reaction

conditions (Table 2, entry 9). Similarly, under the same reaction conditions, 4-dimethylamino benzaldehyde gave poor product yield (Table 2, entry 10). This lower yield might be due to the axial coordination of the amino group in 4-dimethylamino benzaldehyde. Alicyclic aldehyde such as cyclohexane aldehyde reacted efficiently and gave higher yield of the desired olefin (Table 2, entry 11).

Table 2: rGO/hemin catalyzed olefination of aldehydes.^a

Entry	Substrate	Product	Yield (%) ^{b)}	E/Z ratio ^{c)}
1			92	7:1
2			94	4:1
3			93	5:1
4			87	3:1
5			93	5:1
6			85	1:4
7			84	1:3
8			65	1:4
9		-	-	-
10			28	3:1
11			92	5:1

^aReaction conditions: aldehyde (1 mmol), EDA (1.2 mmol), Ph₃P (1.1 mmol), catalyst (1 mol%, 0.01 mmol), toluene (5 ml) at 80 °C under N₂ atmosphere; ^bIsolated yields; ^cE/Z ratio calculated by ¹H NMR.

Reusability of the solid catalyst is one of the most important criteria to make it viable at an industrial scale. To study the reusability of the heterogeneous rGO/hemin catalyst, the olefination of benzaldehyde was studied under optimized reaction conditions. After completion of the reaction, the catalyst was separated by simple filtration and the recovered catalyst was used for subsequent five cycles using benzaldehyde as model substrate. In all cases, the product yield as well as trans-selectivity of the product remained almost the same (Fig. 5). These results confirmed that the developed catalyst was highly stable and can be reused for several runs without any significant change in its catalytic activity. Moreover, the iron content in the recovered catalyst after five runs was found to be almost similar (6.5 wt%) to that of fresh catalyst (6.8 wt%). Furthermore, to ascertain the leaching, a toluene solution of the catalyst was refluxed for 12 h. After separating the catalyst, the obtained filtrate was

charged with substrates i.e. benzaldehyde (1 mmol), Ph₃P (1.1 mmol) and EDA (1.2 mmol) and continued the reaction under refluxing condition for 12 h. No conversion of benzaldehyde was observed, which indicated that the developed catalyst was quite stable and did not show any leaching. These findings further establish the truly heterogeneous nature of the rGO/hemin catalyst.

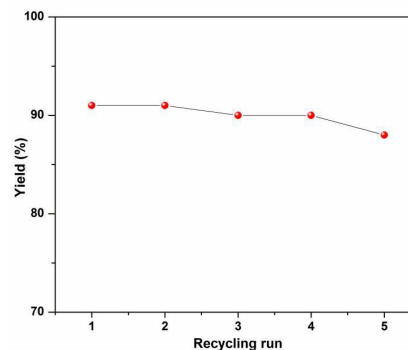


Fig. 5: Recycling experiments.

To investigate the structural and chemical changes of the rGO/hemin catalyst after catalysis, the recovered catalyst after the fifth recycling run was characterized with FTIR, SEM, UV and TGA (Fig. 6). FTIR spectrum of the recycled catalyst showed similar bands like the freshly synthesized catalyst (Fig. 6a). Similarly, the crumpled and erupted structure of the recycled catalyst suggested that the morphology of catalyst remained intact after the catalytic reactions (Fig. 6b). Also no obvious changes were observed in the UV-visible spectrum of the recycled catalyst as compared to that of fresh catalyst (Fig. 6c). Finally, TGA analysis of recycled catalyst (Fig. 6d) suggested that the recycled catalyst was thermally stable and showed similar degradation pattern as freshly synthesized catalyst.

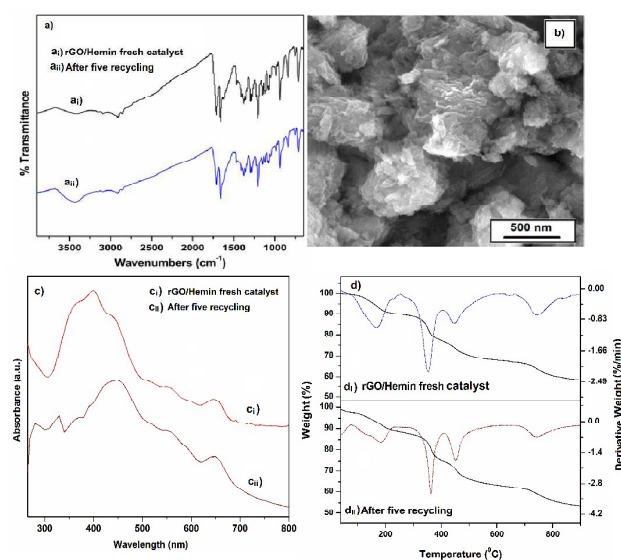
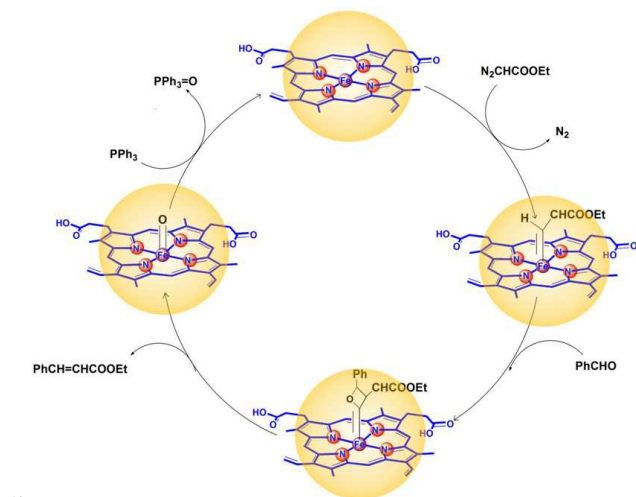


Fig. 6: a) FTIR spectra of rGO/hemin i) fresh catalyst, ii) after five recycling experiments, b) FE-SEM image of recovered rGO/hemin, c) UV-Vis spectra of rGO/hemin: i) fresh catalyst, ii) after five recycling experiments, d) TGA thermograms: i) fresh rGO/hemin, ii) after five recycling experiments.

Although the exact mechanism of the reaction is not clear at this stage, in analogy to the existing report by Woo et al.,^{3b,16} it is assumed that the reaction involves the transfer of carbene generated from ethyldiazoacetate to phosphorous to give phosphazene in the presence of hemin. In the subsequent step, the phosphazene reacts with aldehyde to yield the corresponding olefin in a similar way to Wittig reaction (Scheme 3).



Scheme 3: Possible mechanism of olefination of aldehydes over rGO/hemin.

Conclusion

In conclusion, an efficient and simple method has been described for the synthesis of rGO/hemin hybrid by the treatment of graphene oxide with hemin under ultrasonication for 5 h. FTIR, UV-Vis and TGA measurements confirmed GO reduction and hemin incorporation to yield rGO/hemin hybrid material. The resulting rGO/hemin was successfully used as a selective catalyst for the olefination of various aldehydes. The synthesized catalyst showed the property of both hemin as well as of graphene. Graphene provided large surface area to the substrate, supported hemin through π - π interactions, and increased the active sites on the surface. Due to the synergistic effect of both components, rGO/hemin hybrid catalyst exhibited high and excellent yields of cinnamates from the corresponding aldehydes as compared to the well established homogeneous catalytic systems. Moreover, the catalyst was very stable and can be reused several times without any activity loss.

Experimental

Material

Graphite flakes, iron protoporphyrin IX (hemin) and hydrazine monohydrate were purchased from Sigma-Aldrich. Dichloromethane, potassium permanganate (99.0%), sodium nitrate (99%), concentrated sulphuric acid, hydrogen peroxide (30%), hydrochloric acid (35%), methanol, ethanol, dimethylformamide (DMF) and HPLC

grade water were purchased from MERCK India. All the chemicals and solvents were of analytical grade and used as received.

Characterization

Fourier Transform Infrared (FTIR) spectra were recorded on a Perkin-Elmer spectrum RX-1 IR spectrophotometer using potassium bromide window. UV-Visible absorption spectra of hemin and rGO/hemin in DMF were collected on a Perkin Elmer lambda-19 UV-VIS-NIR spectrophotometer using a 10 mm quartz cell. Thermal stability of samples was evaluated by thermogravimetric analyses (TGA) using a thermal analyzer TA-SDT Q-600. Analysis was carried out in the temperature range of 40 to 800 °C under nitrogen flow with a heating rate of 10 °C/min. The iron content of the hybrid rGO/hemin catalyst was measured on Inductively Coupled Plasma Atomic Emission Spectrometer (ICP-AES, DRE, PS-3000UV, Leeman Labs Inc, USA). For ICP-AES, 0.05 g of catalyst was leached out using Conc. HNO₃ and final volume was made up to 10 ml by adding distilled water.

2.2 Synthesis of rGO/hemin nanocomposite¹¹

Hemin functionalized reduced graphene oxide (rGO/hemin) hybrid was synthesized by following our previously reported method.¹¹ Graphene oxide was synthesized by following the modified Hummer's method.¹⁷ For the synthesis of rGO/hemin/catalyst, 0.75 mL (10 mM) of hemin was dissolved in DMF which was further added to a homogeneous suspension of GO (0.75 mL, 0.5 mg mL⁻¹) in distilled water and ultrasonicated at 130 kHz in a Fisher, Loughborough, Leicester, UK Transonic TI-H-10 ultrasonication bath for 5 h at 50 °C. The precipitate was separated by centrifugation at 14000 rpm for 1 h, washed 3 times with water and dried in an oven at 60 °C for 6 h.

2.3 Typical experimental procedure for olefination of aldehydes

In a 10 mL Schlenk tube, placed in a preheated oil bath at 80 °C, was added aldehyde (1 mmol), ethyldiazoacetate (1.2 mmol), triphenylphosphine (1.2 mmol) and catalyst (1 mol %) in toluene (5 mL) under a nitrogen atmosphere. The resulting mixture was stirred as indicated in Table 2. After being cooled the mixture at room temperature, the catalyst was recovered from the reaction mixture *via* centrifugation. The obtained filtrate was concentrated under reduced pressure and purified by column chromatography using hexane/ethyl acetate (15:1) to give pure olefin. The yields of the isolated products are given in Table 2. The regioselectivity of the products was determined by ¹H NMR.

Acknowledgements

Authors are thankful to Director IIP for granting permission to publish these results. PK is thankful to CSIR New Delhi for providing research fellowship. CJ kindly acknowledges CSIR, New Delhi for providing technical HR under XII five year projects. A.B., S.S. and R.B. acknowledge financial support from the Centre National de la Recherche Scientifique (CNRS), The Lille1 University and the Nord

Pas de Calais region.

Notes and references

^aChemical Sciences Division, CSIR-Indian Institute of Petroleum,

Dehradun-248005, India

Tel. 91-135-2525788; Fax: 91-135-2660202; Email:

suman@iip.res.in

^bAnalytical Sciences Division, CSIR-Indian Institute of Petroleum,
Dehradun-248005, India

^cInstitut d'Electronique, de Microélectronique et de

Nanotechnologie (IEMN), UMR CNRS 8520, Université Lille1,

Avenue Poincaré-BP60069, 59652 Villeneuve d'Ascq Cédex, France

1. a) G. Wittig and G. Geissler, *Justus Liebigs Ann. Chem.*, 1953, **580**, 44–57; b) G. Wittig and U. Schöllkopf, *Chem. Ber.*, 1954, **87**, 1318–1330; c) B. E. Maryanoff and A. B. Reitz, *Chem. Rev.*, 1989, **89**, 863–927; d) V. K. Aggarwal, J. R. Fulton, C. G. Sheldon and J. de Vicente, *J. Am. Chem. Soc.*, 2003, **125**, 6034–6035.
2. a) L. K. Woo and D. A. Smith, *Organometallics*, 1992, **11**, 2346–2348; b) H. Lebel, V. Paquet, *Org. Lett.*, 2002, **4**, 1671–1674.; c) O. Fujimura and T. Honma, *Tetrahedron Lett.*, 1998, **39**, 625–626. d) W. A. Herrmann, P. W. Roesky, M. Wang and W. Scherer, *Organometallics*, 1994, **13**, 4531–4535.
3. a) Y. Chen, L. Huang, M. A. Ranade, and X. P. Zhang, *J. Org. Chem.*, 2003, **68**, 3714–3717; b) G. A. Mirafzal, G. Cheng and L. K. Woo, *J. Am. Chem. Soc.*, 2002, **124**, 176–177.
4. G. Zhang and P. K. Dasgupta, *Anal. Chem.*, 1992, **64**, 517–522.
5. a) M. K. Meffert, J. E. Haley, E. M. Schuman, H. Schulman and D. V. Madison, *Neuron*, 1994, **13**, 1225–1233; b) Y. Zang, J. Lei, L. Zhang and H. Ju, *Anal. Chem.*, 2014, **86**, 12362–12368; c) Q. Wang, Y. Song, H. Xie, Y. Chai, Y. Yuan and R. Yuan, *Chem. Commun.*, 2015, **51**, 1255–1258; d) G.-C. Han, X.-Z. Feng, Z. Chen, *Int. J. Electrochem. Sci.*, 2015, **10**, 3897–3913.
6. a) B. Meunier, *Chem. Rev.*, 1992, **92**, 1411–1456; b) R. D. Arasasingham, A. L. Balch, C. R. Cornman and L. Latos-Grazynski, *J. Am. Chem. Soc.*, 1989, **111**, 4357–4363; c) C. K. Chang and M. Kuo, *J. Am. Chem. Soc.*, 1979, **101**, 3413–3415.
7. a) C.-M. Che, V. K.-Y. Lo, C.-Y. Zhou and J.-S. Huang, *Chem. Soc. Rev.*, 2011, **40**, 1950–1975; b) M. C. A. F. Gotardo, A. A. Guedes, M. A. Schiavon, N. M. Jose, I. V. P. Yoshida and M. D. Assis, *J. Mol. Catal. A.*, 2005, **229**, 137–143; c) E. M. Serwickaa, J. Poltowicza, K. Bahranowski, Z. Olejniczak, W. Jones, *Appl. Catal. A*, 2004, **275**, 9–14.
8. a) C. N. R. Rao, A. K. Sood, K. S. Subrahmanyam and A. Govindaraj, *Angew. Chem. Int. Ed.*, 2009, **48**, 7752 – 7777; b) D. R. Dreyer, S. Park, C. W. Bielawski and R. S. Ruoff, *Chem. Soc. Rev.*, 2010, **39**, 228–240.
9. a) T. Xue, S. Jiang, Y. Qu, Q. Su, R. Cheng, S. Dubin, C.-Y. Chiu, R. Kaner, Y. Huang and X. Duan, *Angew. Chem. Int. Ed.*, 2012, **51**, 3822 –3825; b) Y. Guo, J. Li and S. Dong, *Sens. Actuators B*, 2011, **160**, 295– 300; c) C. Xu, J. Li, X. Wang, J. Wang, L. Wan, Y. Li, M. Zhang, X. Shang and Y. Yang, *Mater. Chem. Phys.*, 2012, **132**, 858– 864; d) Y. Guo, L. Deng, J. Li, S. Guo, E. Wang and S. Dong, *ACS Nano*, 2011, **5**, 1282–1290; e) C. X. Guo, Y. Lei and C. M. Li, *Electroanalysis*, 2011, **23**, 885 – 893; f) H. L. Zou, B. L. Li, H. Q. Luo and N. B. Li, *Sens. Actuators B*, 2015, **207**, 535–541.
10. a) Y. Li, X. Huang, Y. Li, Y. Xu, Y. Wang, E. Zhu, X. Duan and Y. Huang, *Sci. Rep.*, 2013, **3**, 1787–1793; b) Y. Zhang, Z. Xia, H. Liu, M.J. Yang, L.L. Lin and Q.Z. Li, *Sens. Actuators B*, 2013, **188**, 496–501.
11. R. Oprea, S. F. Peteu, P. Subramanian, W. Qi, E. Pichonat, H. Happy, M. Bayachou, R. Boukherroub and S. Szunerits, *Analyst*, 2013, **138**, 4345–4352.
12. S. Bi, T. Zhao, X. Jia and P. He, *Biosens. Bioelectron.*, 2014, **57**, 110–116.
13. X. Lv and J. Weng, *Sci. Rep.*, 2013, **3**, 3285.
14. C. Xu, J. Li, X. Wang, J. Wang, L. Wan, Y. Li, M. Zhang, X. Shang and Y. Yang, *Mater. Chem. Phys.*, 2012, **132**, 858–864.
15. M. Shindo, Y. Sato and K. Shishido, *J. Org. Chem.*, 2000, **65**, 5443–5445.
16. a) G. Cheng, G. A. Mirafzal and L. K. Woo, *Organometallics*, 2003, **22**, 1468–1474; b) C. G. Hamaker, J.-P. Djukic, D. A. Smith and L. K. Woo, *Organometallics*, 2001, **20**, 5189–5199.
17. W. S. Hummers and J. R. E. Offerman, *J. Am. Chem. Soc.*, 1958, **80**, 1339.

Graphene/hemin hybrid material as efficient green catalyst for stereoselective olefination of aldehydes

Chetan Joshi, Pawan Kumar, Babita Behera, Alexandre Barras, Sabine Szunerits, Rabah Boukherroub and Suman L. Jain

